Journal of Power Sources 196 (2011) 1503–1507

Contents lists available at ScienceDirect

Journal of Power Sources

journal homepage: www.elsevier.com/locate/jpowsour

Short communication

Characteristics and structural change of layered polysilane (Si_6H_6) anode for lithium ion batteries

Yoko Kumai*, Soichi Shirai, Eiichi Sudo, Juntaro Seki, Hirotaka Okamoto, Yusuke Sugiyama, Hideyuki Nakano

Toyota Central R&D Labs., Inc., 41-1 Yokomichi, Nagakute, Aichi 480-1192, Japan

ARTICLE INFO

Article history:
Received 1 June 2010
Received in revised form 16 August 2010
Accepted 17 August 2010
Available online 21 August 2010

Keywords:
Silicon nanosheet
Layered polysilane
Electrode
Lithium ion battery
Raman spectroscopy

ABSTRACT

Layered polysilane (Si_6H_6) has a graphite-like structure with higher capacity than crystalline silicon. The rate of increase of the thickness of a layered polysilane electrode after 10 charge–discharge cycles was smaller than that for a Si powder electrode, although the layered polysilane electrode has higher capacity. The structural changes of electrochemically lithiated and delithiated layered polysilane at room temperature were studied using scanning electron microscopy, X-ray diffraction and Raman spectroscopy. Layered polysilane became amorphous by insertion of lithium to 0 V, whereas insertion of lithium into crystalline silicon produces $Li_{15}Si_4$. Layered polysilane maintained an amorphous state during lithium insertion and deinsertion, whereas silicon changed between $Li_{15}Si_4$ and amorphous Li_xSi, which explains the smaller volume change of a layered polysilane electrode compared with a Si powder electrode.

1. Introduction

Carbon based materials are still used as anodes for lithium ion batteries, although the theoretical capacity of 372 mAh g^{-1} is not sufficient; therefore, there is an intensive research effort to identify higher capacity anode materials. Silicon based materials have attracted much attention, because $Li_{15}Si_4$ exhibits the highest theoretical capacity of 3579 mAh g^{-1} at room temperature [1,2]. However, $Li_{15}Si_4$ has a major problem in that its volume changes upon intensive discharge–charge cycling. In an attempt to solve this problem, Si anodes have been prepared with micron-sized particles [3], nanosized particles [4,5], and thin films [6] of silicon. The change in volume is accompanied by a change of structure. It has been reported that the crystalline Si electrode changes to amorphous Li_xSi by a first electric discharge to 50 mV, followed by a change to $Li_{15}Si_4$ by discharge to 0 mV. Delithiation of the $Li_{15}Si_4$ phase results in the formation of amorphous Si [1].

Layered polysilane has a hexagonal layered structure (Fig. 1) that consists of corrugated Si(1 1 1) planes in which the Si_6 rings are interconnected (referred to as a silicon nanosheet). The planar size and thickness of the silicon nanosheets are in the range of dozens of micrometers and nanometers, respectively. Thus, layered polysilane has a graphite-like structure that is constructed of layered carbon sheets. It is synthesized by reacting powdered $CaSi_2$ with aqueous HCl at −30 °C and rinsing with aqueous HF, as reported by Dahn et al. [7]. We believe that layered polysilane should have a higher capacity than Si powder, due to the spaces between the silicon nanosheets that could act as pathways for Li ions.

Here we report the capacitance characteristics and structural changes of layered polysilane during electrochemical lithium insertion and deinsertion (discharge/charge).

2. Experimental

2.1. Synthesis of layered polysilane electrode and Si powder electrode

Electrodes were prepared with 70 wt% active material (layered polysilane or Si nanopowder (<100 nm particle size, Aldrich)), 25 wt% carbon black (TB5500, Tokai Carbon, Japan), and 5 wt% polytetrafluoroethylene (F-104, Daikin, Japan). 10 mg of electrode material was placed on a stainless steel mesh and dried at 110 °C for 2 h under vacuum.

* Corresponding author at: Toyota Central R&D Labs., Inc., Frontier Research Center, 41-1 Yokomichi, Nagakute, Aichi 480-1192, Japan. Tel.: +81 561 71 7961; fax: +81 561 63 6507.
E-mail addresses: kumai@mosk.tytlabs.co.jp (Y. Kumai), shirai@mosk.tytlabs.co.jp (S. Shirai), eiichi-s@mosk.tytlabs.co.jp (E. Sudo), e1302@mosk.tytlabs.co.jp (J. Seki), h-okamoto@mosk.tytlabs.co.jp (H. Okamoto), e1521@mosk.tytlabs.co.jp (Y. Sugiyama), hnakano@mosk.tytlabs.co.jp (H. Nakano).

0378-7753/$ – see front matter © 2010 Elsevier B.V. All rights reserved.
doi:10.1016/j.jpowsour.2010.08.040

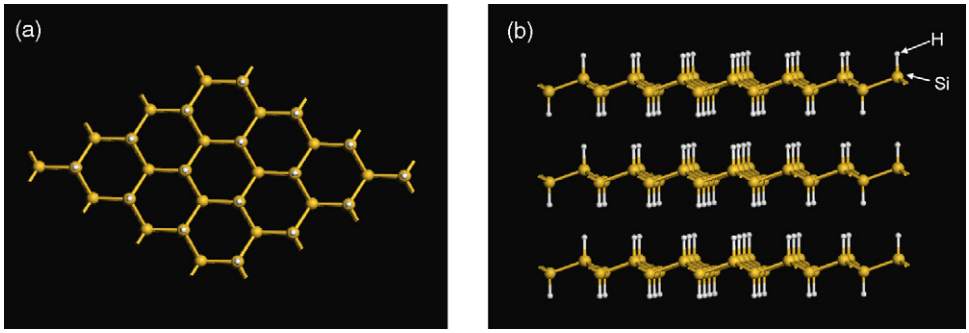

Fig. 1. Schematic model of layered polysilane in the (a) top view and (b) side view.

2.2. Electrochemical analysis

The electrodes were cycled vs. a lithium anode using bipolar system cell hardware (Tomcell Japan) with an electrolyte of 1 M $LiPF_6$ in ethylene carbonate/diethyl carbonate (EC/DEC; 3:7 (w/w), Toyama Pure Chemical Industries, Japan) and a porous polyethylene film (E25MMS, Tonen Chemical, Japan) as a separator. These cells were prepared in a dry argon-filled glove box. The cells were cycled (HJR-1010SM8, Hokuto Denko, Japan) at a constant current of 0.7 mA (0.1 A g^{-1} Si) and with a voltage cut-off range was 0–1.0 V. After cycling, the cells were disassembled in the glove box and the electrodes were rinsed with DEC (Kishida Chemical Co., Japan) and dried in the glove box for characterization using scanning electron microscopy (SEM), X-ray diffraction (XRD) and Raman spectroscopy.

2.3. Scanning electron microscopy

The electrode microstructures were examined using SEM (S-5500, Hitachi). Samples were transferred to the SEM in an Ar-filled chamber.

2.4. X-ray diffraction

X-ray diffraction (RINT-TTR, Rigaku, Japan) analyses employed Cu Kα radiation (50 kV, 300 mA) with slits DS = 0.5°, SS = 0.5°, and RS = 0.15 mm. The samples were placed on a glass substrate in a gastight sample holder containing dry argon to prevent exposure to the air.

2.5. Raman spectroscopy and theoretical calculations

Raman spectroscopy (NRS-3300, Jasco, Japan) was conducted using a 785 nm excitation wavelength, 20× magnification objective lens, 30 s exposure time, and 2.2 mW laser power. Samples were placed in a gastight sample holder containing dry argon.

Theoretical calculations were performed according to the *ab initio* quantum chemistry method. The layered polysilane was first modeled as $Si_{24}H_{36}$ (Fig. 2) and the molecular structure was optimized. Second-derivative calculations were then carried out for vibrational analysis. Density functional theory (DFT) was employed with the B3LYP hybrid exchange-correlation functional. Pople's 6-31G(d) was used as the basis set. The calculated vibrational frequencies were multiplied by 0.9613, which is the scale factor for B3LYP/6-31G(d). All calculations were performed using the Gaussian 03 program package [8].

3. Results and discussion

Fig. 3 shows the results of galvanostatic discharge–charge measurements and the capacities of the layered polysilane and Si powder electrodes. A large amount of irreversible capacity appeared in the first cycle for both electrodes. The first Coulombic efficiency for polysilane (37%) was larger than that for silicon (31%). The absence of solid electrolyte interface (SEI) formation in the Si electrode has previously been reported [9], whereas the carbon electrode always exhibits a voltage plateau near 0.8–1.0 V as a result of SEI formation. Therefore, the voltage plateau near 1.0 V that appeared for both electrodes is considered to be due to SEI formation from the carbon black in the electrodes. The voltage plateau that appeared only for the layered polysilane electrode near 0.3 V is thought to be the voltage for Si–H bond breaking; however, the evidence and the reason for this is under investigation and will be reported in the near future.

The first charge capacity of the layered polysilane electrode was 1677 mAh g^{-1} and that of the Si powder electrode was 910 mAh g^{-1}. The volumetric capacity of the layered polysilane electrode (2730 Ah L^{-1}) is larger than that of graphite (820 Ah L^{-1}). The volumetric capacity of the layered polysilane electrode was calculated from the absolute specific gravity of layered polysilane (1.5 g cm^{-3}), carbon black (1.9 g cm^{-3}), and polytetrafluoroethylene (2.0 g cm^{-3}). After 10 cycles, the capacity retention of both electrodes was 50%. The thickness of the layered polysilane and Si powder electrodes was increased by 150% and 156%, and the capacities at the 10th cycle were 817 and 464 mAh g^{-1}, respectively. The layered polysilane electrode had a lower rate of volume increase than the Si powder electrode by the absorption of Li. The reason for this is not yet clear; however, it may be due to the influence of the space between the silicon nanosheets. The diffusion coefficient of Li can be expressed by Eq. (1) [10]. The apparent chemical diffusion coefficients of Li for the first charge in the layered polysilane and Si powder electrodes were 2.3×10^{-9} and 4.9×10^{-10} cm^2 s^{-1}, respectively; the diffusion of Li ions was faster in the layered polysilane electrode than in the Si powder electrode.

$$\sigma = \frac{V_M(dE/dx)}{nFA(2D)^{1/2}} \quad (1)$$

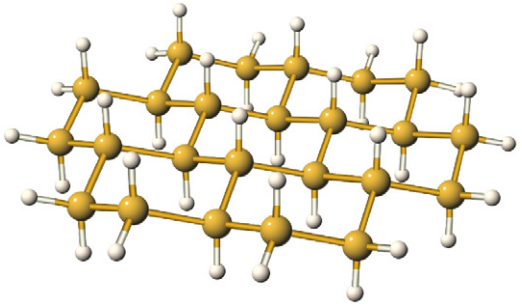

Fig. 2. Model of layered polysilane ($Si_{24}H_{36}$) used for Raman calculations.

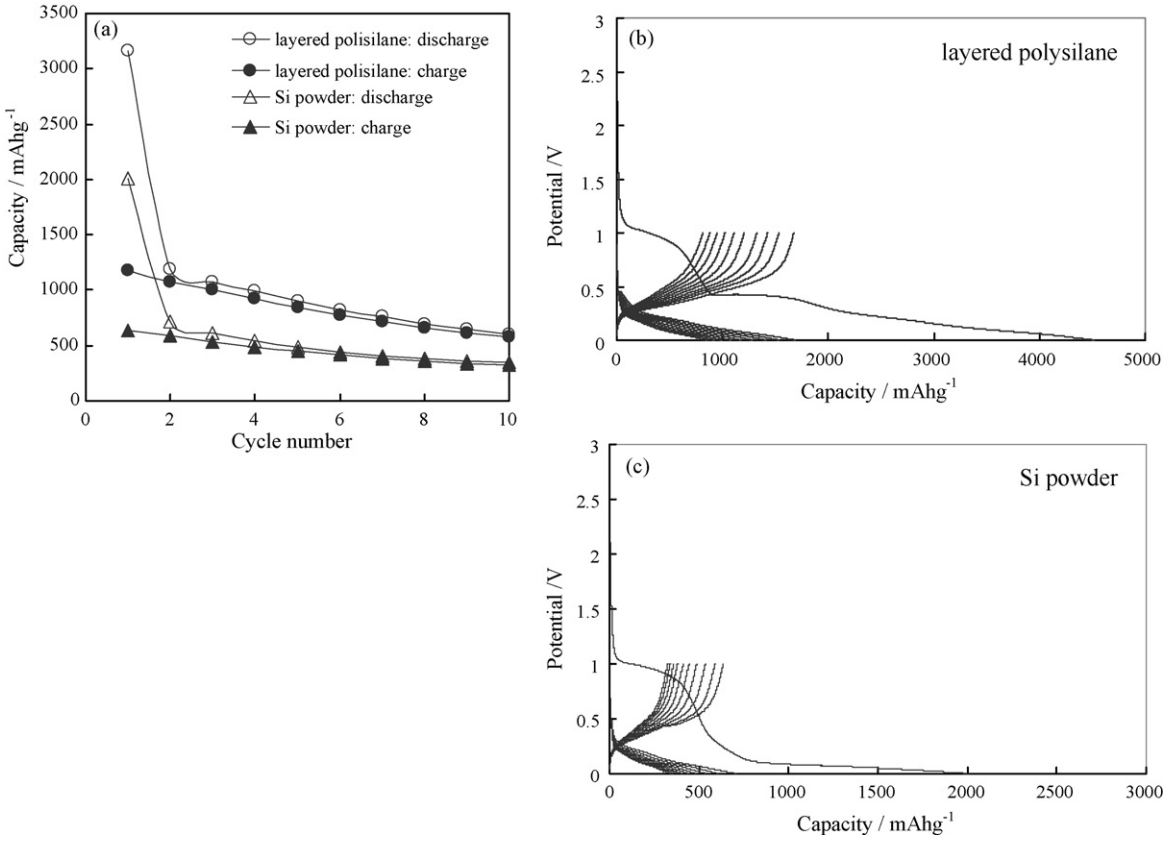

Fig. 3. Charge and discharge capacities of (a) layered polysilane and Si powder electrode. with cycling. Charge and discharge curves of the (b) layered polysilane and (c) Si powder electrodes.

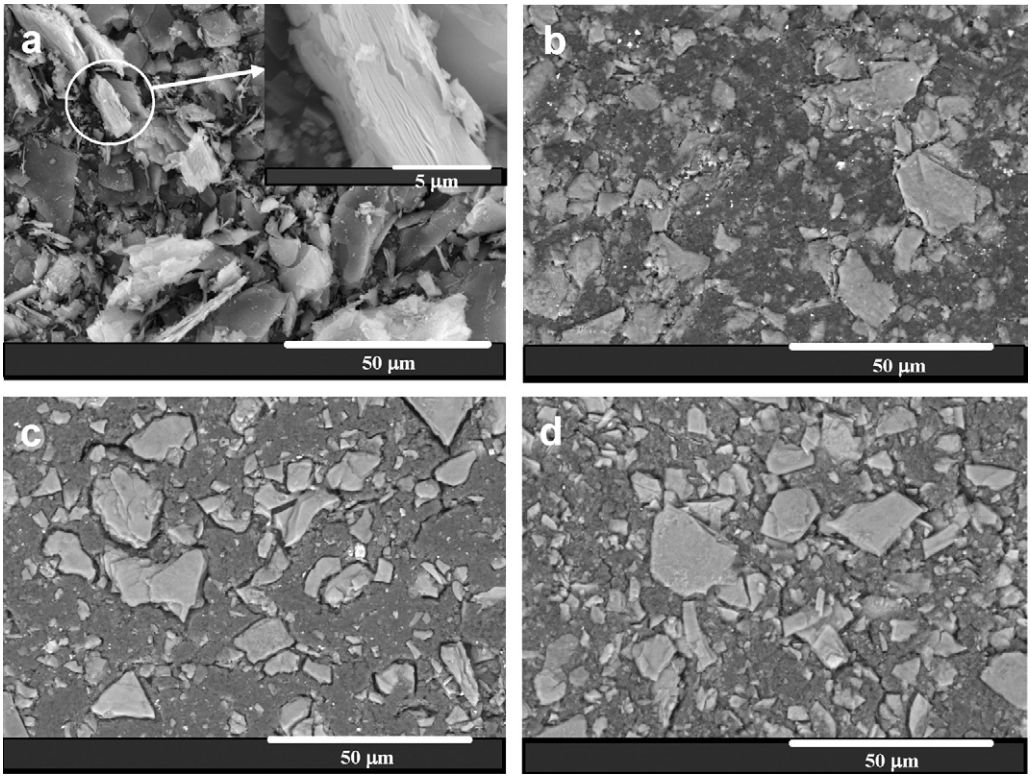

Fig. 4. SEM images of layered polysilane and layered polysilane electrodes. (a) Secondary electron image of layered polysilane. Backscattered electron images of layered polysilane electrodes after (b) the 1st discharge, (c) 10 discharge–charge cycles, and (d) 10 discharge–charge cycles followed by discharge.

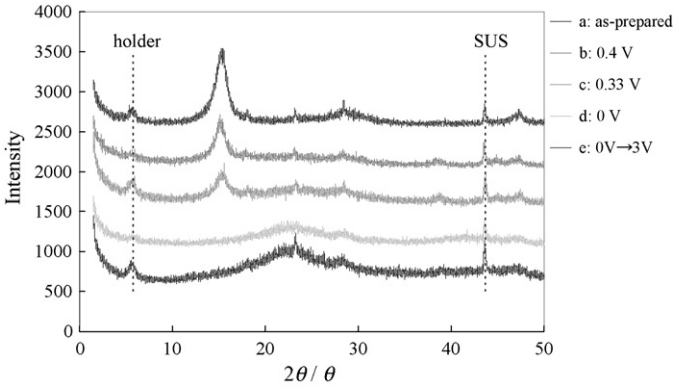

Fig. 5. XRD patterns of layered polysilane electrodes (5.8°: sample holder, 43.7°: stainless steel (SUS) mesh).

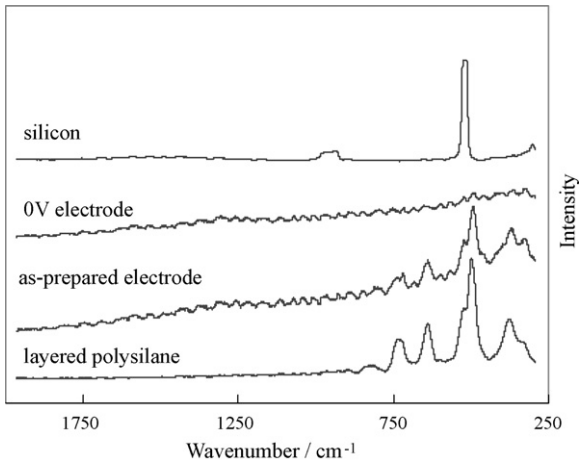

Fig. 6. Raman spectra of layered polysilane, layered polysilane electrodes and bulk silicon (reference).

where V_M is the molar volume of the host (cm mol^{-1}); dE/dx is the slope of the coulometric titration curve vs. mobile ion concentration x at each x value (V); n is the electronic number of the reaction (1); F is the Faraday constant (96,485 C mol^{-1}); A is the surface area of the electrode (cm^2); σ is the Warburg coefficient.

Fig. 4 shows SEM images of the layered polysilane powder and layered polysilane electrode after the first discharge to 0 V, 10 cycle discharge–charge, and 10 cycle discharge–charge followed by discharge to 0 V. The particle sizes of the layered polysilane (Fig. 4(a)) were from several to dozens of micrometers, and the cross-section indicated a layered structure (Fig. 4(a) inset). The layered polysilane particles are 'islands' surrounded by the carbon black in the electrode (Fig. 4(b)–(d)). After the first discharge (lithiation), the layered polysilane in the electrode made increased contact with the carbon black (Fig. 4(b)). However, after 10 discharge–charge cycles (delithiation), crevices between the layered polysilane particles and the carbon black became evident (Fig. 4(c)). The crevices seem to be due to the volume expansion and contraction of the layered polysilane particles by discharge and charge, which is one of the reasons that the capacity is decreased with increasing cycle number. The crevices evident in the 10 discharge–charge cycled electrode followed by discharge to 0 V (Fig. 4(d)) were smaller than those in the 10 discharge–charge cycled electrode, due to an increase of the volume by lithiation.

The electrochemical mechanism of the layered polysilane was investigated by *ex situ* XRD measurements of the electrodes after the first discharge process (Fig. 5). The as-prepared electrode (Fig. 5a) had two peaks at 15.5° and 47.6°, which were indexed as (0 0 1) and (1 1 0), respectively, on the basis of layered polysilane with a hexagonal unit cell with a = 3.83 and c = 5.70 Å. The (0 0 1) peak was also detected for the electrode discharged to 0.4 V (Fig. 5b) and 0.33 V (Fig. 5c), and their half-widths were the same at 1.37°. This result indicates that the layered polysilane underwent no structural change until 0.33 V, although there are two steps (ca. 1.0 V and 0.33 V in Fig. 3b) in the galvanostatic curve. The (0 0 1) peak was not detected for the electrode discharged to 0 V and only a broad reflection peak was detected at 25° (Fig. 5d). This suggests that the periodicity of the silicon nanosheets changed to the amorphous Li_xSi phase [7]. The electrode discharged to 0 V followed by charging to 3 V (Fig. 5e) had a broad reflection peak at 25° and no peak at 15.5°, which indicates that the periodicity of the Si nanosheets was not recovered, despite delithiation of the layered polysilane.

The local silicon structure of the layered polysilane was investigated using Raman spectroscopy. Fig. 6 shows Raman spectra of the layered polysilane, the as-prepared layered polysilane electrode, the electrode discharged to 0 V and bulk silicon (as reference). The spectrum of layered polysilane has five prominent peaks at 382.6, 501.8, 643.8, 737.7 and 835.4 cm^{-1}, which is different from that for bulk silicon, and reflects the unique structure of the material. However, to the authors' knowledge, there are no reports of the Raman spectroscopy of layered polysilane; therefore, theoretical *ab initio* quantum chemical calculations were conducted. The computationally obtained spectrum is given in Fig. 7. In addition to a number of smaller peaks, four intense peaks were obtained at 313.3, 472.4, 742.7 and 886.7 cm^{-1}, which correspond to the experimental peaks observed at 382.6, 501.8, 737.7 and 835.4 cm^{-1}. As a result of detailed analysis, the peaks at 313.3 and 472.4 cm^{-1} were both attributed to the Si–Si bending mode (Fig. 8a), while the peaks at 742.7 and 886.7 cm^{-1} were assigned to the Si–H bending (Fig. 8b) and SiH_2 scissoring modes (Fig. 8c), respectively. Although there was no intense peak that corresponded to the experimentally observed peak at 643.8 cm^{-1}, several small peaks were observed in the range of 620–690 cm^{-1}, which correspond to the Si–H bending mode. Therefore, it was concluded that peaks below and above 600 cm^{-1} originate from Si–Si and Si–H vibrations, respectively. In the computationally obtained spectrum, the peak of Si–H (742.7 cm^{-1}) has almost the same intensity as that of SiH_2 (886.7 cm^{-1}); however, in the experimental spectra, the intensity of the Si–H (737.7 cm^{-1}) peak is approximately five times that of the SiH_2 (835.4 cm^{-1}) peak. This discrepancy can be attributed to the size of the model employed in the calculations, which contains the same number (twelve) of Si–H and SiH_2, while in the layered polysilane, the number of Si–H is relatively larger than SiH_2, because SiH_2 is present only at the sides of the silicon nanosheet.

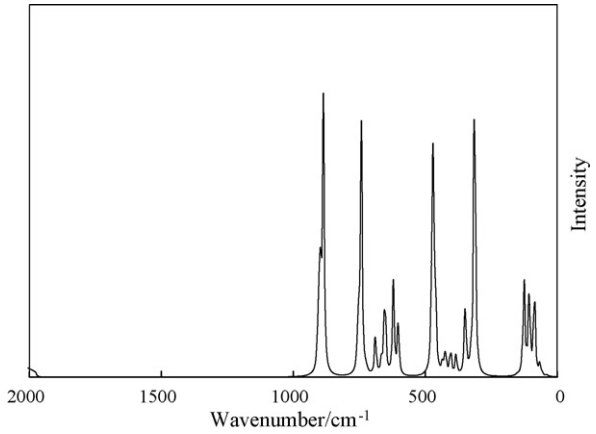

Fig. 7. Computationally obtained Raman spectrum.

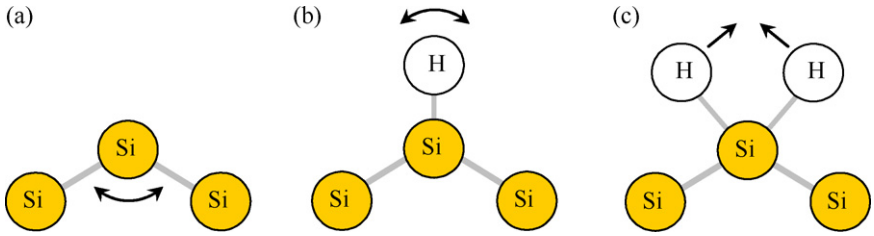

Fig. 8. Models depicting (a) Si–Si bending, (b) Si–H bending, and (c) SiH_2 scissoring modes.

The five experimental Raman peaks were also detected for the as-prepared electrode, but not from the electrode discharged to 0 V, which suggests the collapse of the Si–Si and Si–H bonds. This result indicates that Si–Li bond formation occurred by discharge to 0 V. From the results of XRD measurements and Raman spectroscopy, we concluded that the layered polysilane discharged to 0 V became amorphous Li_xSi.

4. Conclusions

The electrical capacitance and structural changes of a layered polysilane electrode were examined. The layered polysilane electrode has higher capacitance and a smaller change in volume than the Si powder electrode during the lithium insertion/deinsertion process. The layered polysilane became amorphous Li_xSi after the first discharge to 0 V and remained amorphous Li_xSi during discharge–charge cycling, whereas Si powder was changed to crystalline $Li_{15}Si_4$ after the first discharge to 0 V, and then changed between $Li_{15}Si_4$ and an amorphous Li_xSi during discharge–charge cycling. One of the reasons for the smaller volume change of the layered polysilane electrode than that for the Si powder electrode is the lack of phase change in the layered polysilane electrode after the first discharge. Therefore, it is concluded that layered polysilane is a potential candidate anode material for lithium ion rechargeable batteries.

References

[1] M.N. Obrovac, L. Christensen, Electrochem. Solid-State Lett. 7 (2004) A93–A96.
[2] T.D. Hatchard, J.R. Dahn, J. Electrochem. Soc. 151 (2004) A838–A842.
[3] J.H. Ryu, J.W. Kim, Y.E. Sung, S.M. Oh, Electrochem. Solid-State Lett. 7 (2004) A306–A309.
[4] H. Li, X.J. Huang, L.Q. Chen, Z.G. Wu, Y. Liang, Electrochem. Solid-State Lett. 2 (1999) 547–549.
[5] S.Y. Chew, Z.P. Guo, J.Z. Wang, J. Chen, P. Munroe, S.H. Ng, L. Zhao, H.K. Liu, Electrochem. Commun. 9 (2007) 941–946.
[6] J.P. Maranchi, A.F. Hepp, P.N. Kumta, Electrochem. Solid-State Lett. 6 (2003) A198–A201.
[7] J.R. Dahn, B.M. Way, E. Fuller, Phys. Rev. B 48 (1993) 17872–17877.
[8] M.J. Frisch, G.W. Trucks, H.B. Schlegel, G.E. Scuseria, M.A. Robb, J.R. Cheeseman, J.A. Montgomery Jr., T. Vreven, K.N. Kudin, J.C. Burant, J.M. Millam, S.S. Iyengar, J. Tomasi, V. Barone, B. Mennucci, M. Cossi, G. Scalmani, N. Rega, G.A. Petersson, H. Nakatsuji, M. Hada, M. Ehara, K. Toyota, R. Fukuda, J. Hasegawa, M. Ishida, T. Nakajima, Y. Honda, O. Kitao, H. Nakai, M. Klene, X. Li, J.E. Knox, H.P. Hratchian, J.B. Cross, V. Bakken, C. Adamo, J. Jaramillo, R. Gomperts, R.E. Stratmann, O. Yazyev, A.J. Austin, R. Cammi, C. Pomelli, J.W. Ochterski, P.Y. Ayala, K. Morokuma, G.A. Voth, P. Salvador, J.J. Dannenberg, V.G. Zakrzewski, S. Dapprich, A.D. Daniels, M.C. Strain, O. Farkas, D.K. Malick, A.D. Rabuck, K. Raghavachari, J.B. Foresman, J.V. Ortiz, Q. Cui, A.G. Baboul, S. Clifford, J. Cioslowski, B.B. Stefanov, G. Liu, A. Liashenko, P. Piskorz, I. Komaromi, R.L. Martin, D.J. Fox, T. Keith, M.A. Al-Laham, C.Y. Peng, A. Nanayakkara, M. Challacombe, P.M.W. Gill, B. Johnson, W. Chen, M.W. Wong, C. Gonzalez, J.A. Pople, Gaussian 03, Revision E. 01, Gaussian, Inc, Wallingford, CT, 2004.
[9] X. Wu, Z. Wang, L. Chen, X. Huang, Electrochem. Commun. 5 (2003) 935–939.
[10] C. Ho, I.D. Raistrick, R.A. Huggins, J. Electrochem. Soc. 127 (1980) 343–350.